Photon Transmission Method for Studying Void-Closure Kinetics During Coalescence of Hard Latex Particles

ÖNDER PEKCAN, FİGEN KEMEROĞLU

Department of Physics, Istanbul Technical University, 80626, Maslak, Istanbul, Turkey

Received 20 June 1996; accepted 15 December 1996

ABSTRACT: The contribution of viscous flow to void-closure processes during film formation with hard latex particles was studied. Film optical clarity was used to follow the progress of this event. The latex films were prepared from poly(methyl methacrylate) (PMMA) particles and annealed in 10 min time intervals above the glass transition (T_g) temperature. Scanning electron microscopy (SEM) was used to detect the variation in the physical structure of the annealed films. To mimic the latex film-formation process, Monte Carlo simulations were performed for photon transmission through the latex film and the number of transmitted and scattered photons are calculated as a function of the mean free path. A relation for transmitted light intensity, I_{tr} versus void closure (time)$^{1/2}$ ($t^{1/2}$) was derived by using the Vogel–Fulcher viscosity equation. The viscosity constant, B, was produced using this $I_{tr}(t^{1/2})$ relation at various temperatures and found to be 12.8×10^3 K. It is shown that Monte Carlo results justified the $I_{tr}(t^{1/2})$ relation. © 1999 John Wiley & Sons, Inc. J Appl Polym Sci 72: 981–988, 1999

Key words: latex film; void closure; photon transmission; viscous flow

INTRODUCTION

Coalescence of polymer particles is generally described by the formation of a uniform, homogeneous film by the merger of particles. Coalescence of organic polymers is always performed above the glass transition temperature (T_g) and is driven by many different kinds of forces, either intrinsic such as surface tension or externally applied as, e.g., in compression molding. Particle coalescence, in general, requires a combination of physical processes such as deformation, interdiffusion, and stress relaxation, which can be distinguished by two different categories: first, the void-closure process where molecularly contacting interfaces between particles can be established,[1] and, second, interdiffusion of chains across the interface which takes place to establish a uniform distribution of entanglements, which is also called equilibration of the material.[2] The void-closure process is, in fact, a relaxation of mechanical stresses resulting from deformations of particles during neck growth.[3]

Latex films are generally formed by coalescence of submicron polymer particles in the form of a colloidal dispersion, usually in water. The term "latex film" normally refers to a film formed from soft latex particles (T_g below room temperature) where the forces accompanying the evaporation of water are sufficient to compress and deform the particles into transparent, void-free film. However, latex films can also be obtained by compression molding of a film of dried latex powder composed of relatively hard polymers such as polystyrene (PS) or poly(methyl methacrylate) (PMMA) that have their T_g above room temperature. Hard latex particles remain essentially discrete and undeformed during drying. The mechanical properties of such films can be evolved after all solvent has evaporated, by an annealing process which first leads to void closure and then to interdiffusion of chains across particle–particle interfaces.

Correspondence to: O. Pekcan.

Journal of Applied Polymer Science, Vol. 72, 981–988 (1999)
 CCC 0021-8995/99/080981-08

Transmission electron microscopy (TEM) has been the most common technique used to investigate the structure of dried films.[4,5] A pattern of hexagons, consistent with face-centered cubic packing, are usually observed in highly ordered films. When these films are annealed, complete disappearance of the structure is sometimes observed, which is consistent with extensive polymer interdiffusion. Freeze-fracture TEM (FFTEM) was used to study the structure of dried latex films.[6,7] Small-angle neutron scattering (SANS) was used to study latex film formation at the molecular level. Extensive studies using SANS were performed by Sperling and co-workers[8] on compression-molded PS films. The direct nonradiative energy transfer (DET) method was employed to investigate the film-formation processes from dye-labeled hard[9] and soft[10,11] polymeric particles. The steady-state fluorescence (SSF) technique combined with DET was recently used to examine healing and interdiffusion processes in dye-labeled hard latex systems.[12–16]

Determining the rate-limiting step during the film formation from latex is of scientific interest, because it can provide insight into the mechanism of the process. It has been suggested that there are two important components in the process of latex film formation: The first one is the evaporation of the solvent and the second is the deformation of particles leading to void closure.[17,18] Equations were proposed to describe how the time for film formation varies as a function of the temperature of the latex, when each of the steps is rate-limiting.[17]

In this work, since nonaqueous hard latex dispersions are used, deformations of particles leading to void closure is believed to be the rate-limiting step for film formation. Here, we studied the evolution of the transparency of films formed from hard latex particles, by monitoring the photons transmitted from the films during the coalescence of particles, using a UV visible (UVV) spectrophotometer. It was shown that the variation in transparency is related to the variation in transmitted photon intensity (I_{tr}). Isothermal experiments were performed by annealing latex films in equal time intervals and I_{tr} was monitored to study viscous flow during film formation. Increase in I_{tr} intensity by increasing the number of annealing time intervals was attributed to the void-closure process. An equation proposed by Keddie et al.[17] was used to interpret the time dependence of I_{tr} intensity during the void-closure process.

In UVV experiments, hard latex particles having two components were used[19,20]; the major part, PMMA, composes 96 mol % of the material and the minor component, polyisobutylene (PIB) (4 mol %), forms an interpenetrating network through the particle interior,[21,22] which is very soluble in certain hydrocarbon media. A thin layer of PIB covers the particle surface and provides colloidal stability by steric stabilization.

In this article, Monte Carlo simulations were performed to calculate the scattered (N_{sc}) and transmitted (N_{tr}) photon intensities from a rectangular film. Evolution in transparency is modeled by the variation in the mean free path of a photon in latex films at each annealing step. The increase in the optical path of a photon is explained by the void-closure processes due to the neck growth.

EXPERIMENTAL

PMMA–PIB polymer particles were prepared separately in a two-step process in which MMA in the first step was polymerized to low conversion in cyclohexane in the presence of PIB containing 2% isoprene units to promote grafting. The graft copolymer so produced served as a dispersant in the second stage of polymerization, in which MMA was polymerized in a cyclohexane solution of the polymer. Details have been published.[19] A stable spherical dispersion of the polymer particles was produced, ranging in radius from 1 to 3 μm. H-NMR analysis indicated that these particles contain 6 mol % PIB per g of polymer. (These particles were prepared by Mr. B. Williamson in Prof. M. A. Winnik's laboratory in Toronto and provided to us for our use). Latex film preparation was carried out by dispersing particles in heptane in a test tube with a solid content taken as 1%.

In this work, UVV experiments were carried out with isothermally annealed latex film samples. Films were prepared from the dispersion of particles by placing a different number of drops on square glass plates of size of 1×1 cm^2 and allowing heptane to evaporate. Here, we were careful that the liquid dispersion from the droplets covered the whole surface area of the plate and remained there until the heptane was evaporated. Samples were weighed before and after the film casting to determine the film thicknesses.

Latex film samples were isothermally annealed above the T_g of PMMA for 10 min time intervals at 150, 160, 170, 180, 190, and 200°C temperatures. The temperature was maintained within

±2°C during annealing. After annealing, each sample was placed in a Model 160A UV visible spectrophotometer of Shimadzu and UVV absorption was detected between 300 and 400 nm. Another glass plate was used as a standard for all UVV experiments. All measurements were carried out at room temperature. For SEM images, a Hummer VII sputtering system was used for gold coating and the film of the particles was then examined at 10–15 kV in a JEOL JSM-T330 microscope.

VOID-CLOSURE KINETICS

The void-closure kinetics can determine the time for optical transparency and film formation.[17] An expression to relate the shrinkage of spherical void of radius, r, to the viscosity of surrounding medium, η, was derived and is given by the following relation[17]:

$$\frac{dr}{dt} = -\frac{\gamma}{2\eta}\left(\frac{1}{\rho(r)}\right) \tag{1}$$

where γ is surface energy; t, time; and $\rho(r)$, the relative density. It has to be noted that here surface energy causes a decrease in void size and the term $\rho(r)$ varies with the microstructural characteristics of the material, such as the number of voids and the initial particle size and packing. Equation (1) is similar to one which was used to explain the time dependence of the minimum film-formation temperature during latex film formation.[23] If the viscosity is constant in time, integration of eq. (1) gives the relation as

$$t = -\frac{2\eta}{\gamma}\int_{r_0}^{r}\rho(r)\,dr \tag{2}$$

where r_0 is the initial void radius at time $t = 0$.

The temperature dependence of the viscosity of the most amorphous polymers near their T_g can be described by the Vogel–Fulcher (VF)[24,25] equation as

$$\eta = A\exp\left(\frac{B}{T - T_0}\right) \tag{3}$$

where A, B, and T_0 are constants for a given polymer. For most glasses, T_0 is typically about 50 K lower than the T_g. Combining eqs. (2) and (3), the following useful equation is obtained:

$$t = -\frac{2A}{\gamma}\exp\left(\frac{B}{T - T_0}\right)\int_{r_0}^{r}\rho(r)\,dr \tag{4}$$

Equation (4) will be employed to interpret the photon transmission data to explain the void-closure mechanism in following sections.

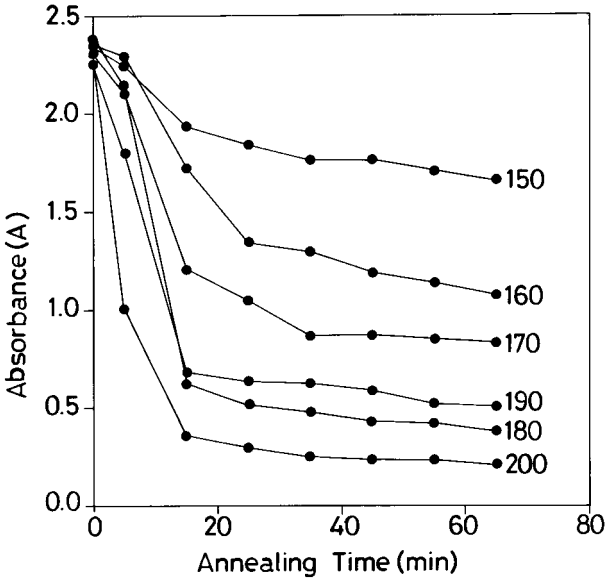

Figure 1 Plot of absorbance A versus annealing time for latex films annealed at temperatures given on each curve in °C.

RESULTS AND DISCUSSION

Optical Clarity and Path of Photons in Latex Films

Absorbance (optical density) (A) of latex films versus annealing time at various temperatures is shown in Figure 1. In these samples, (A) decreased continuously by increasing the number of annealing time intervals. Using the relation $I_{tr} = I_0 \times 10^{-A}$, transmitted photon intensities are obtained and plotted versus annealing time in Figure 2 for various temperatures. It is seen that I_{tr} intensity curves all present an increase as annealing time is increased. This behavior of I_{tr} suggests that latex films become more transparent to photons as they are annealed for longer times. Lower intensities are observed in films annealed at lower temperatures, which indicates that photons cannot be transmitted as good as they are

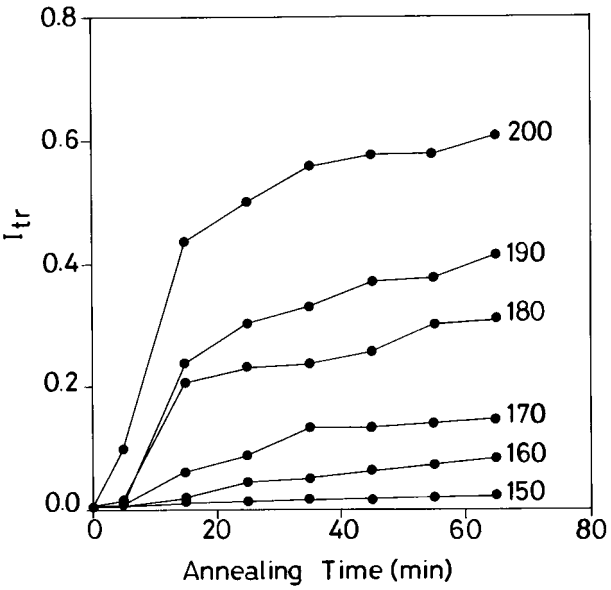

Figure 2 Plot of transmitted photon intensities (I_{tr}) versus annealing time at temperatures given an each curve in °C.

in films annealed at high temperatures. In other words, some photons dissipate or cannot reach the photomultiplier tube after they pass through the films annealed at low temperatures. All I_{tr} curves reach a plateau at long annealing times.

To interpret the time behavior of I_{tr} intensity, a simple rectangular lattice model is used to simulate the latex film-formation process. The rectangular lattice is divided into cubes with side length, a, and the corners of the cubes are taken as a scattering center for photons. a is the distance of a photon between each consecutive collision, which can be defined as the mean free path of a photon during its journey in the lattice. The thickness of the rectangle, d, is taken as a constant; however, the mean free path, $\langle a \rangle$, of a photon is increased to simulate the latex film formation. Here, we simply assumed that as the latex film is annealed the mean free path of a photon is increased due to the void-closure process. The direction of an incident photon is taken perpendicular to the film's front surface and the periodic boundary conditions are applied to the motion of a photon (i.e., photons are not allowed to escape from the sides of the film). The number of photons transmitted from the back surface of the film is called N_{tr} and the number of photons that emerged from the front surface is presented by N_{sc}. Figure 3(a–c) illustrates the path of photons in rectangular lattices with small, medium, and large mean free paths, respectively. Here, the incident number of photons is taken as 3×10^3. Figure 3(a) presents a photon which is scattered from the front surface of the lattice with a small $\langle a \rangle$. Figure 3(b,c) shows the path of photons which are transmitted from the back surface of the lattice with medium and long $\langle a \rangle$ values, respectively. N_{tr} and N_{sc} values are plotted against square of mean free path $\langle a^2 \rangle$ of a photon in Figures 4 and 5, respectively, where numbers on the N_{tr} and N_{sc} curves indicate the percent of trap centers in the lattice which cause the dissipation of photons. Curves with a high percent of trap centers may correspond to the la-

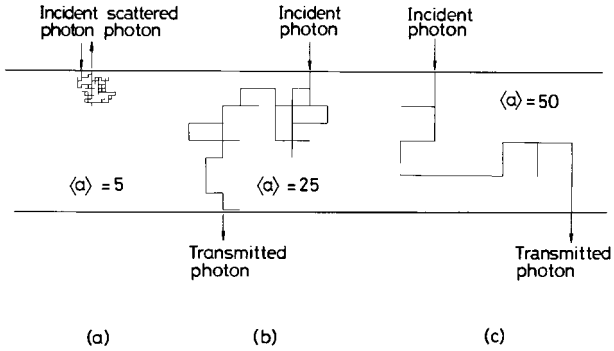

Figure 3 Path of photons in rectangular lattices with (a) small (5), (b) medium (25), and (c) large (50) mean free paths $\langle a \rangle$. The thickness of the rectangular lattice is taken as $d = 200$.

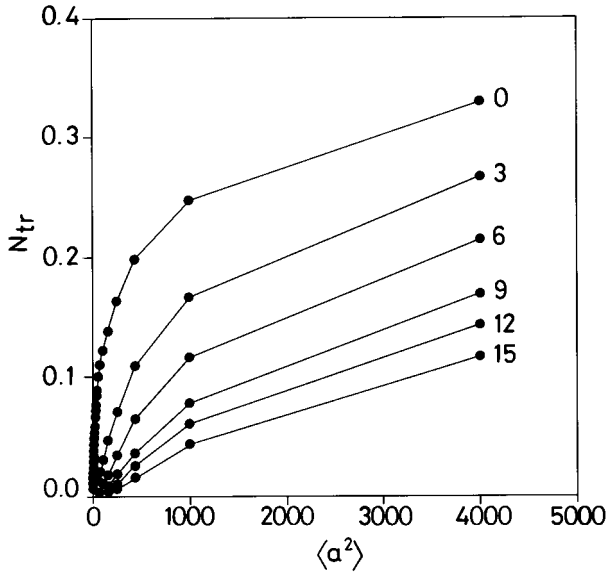

Figure 4 Plot of number of photons, N_{tr}, transmitted from the back surface of the rectangular lattice versus the square of the mean free path $\langle a^2 \rangle$ of a photon. The numbers given on each curve present the percent of trap centers in the lattice.

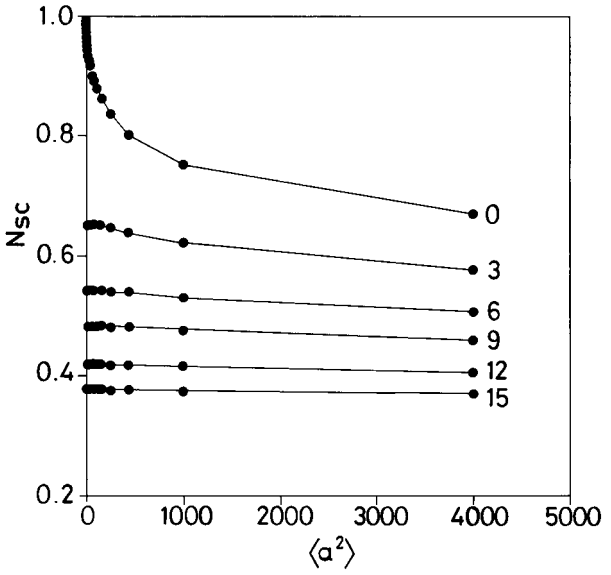

Figure 5 Plot of number of scattered photons, N_{sc}, from the front surface of the rectangular lattice versus $\langle a^2 \rangle$. The numbers given on each curve present the percent of trap centers in the lattice.

tex films annealed at lower temperatures. Here, we assumed that the time evolution of the mean free path obeys the $\langle a^2 \rangle \alpha t$ relation; in other words, the time dependence of N_{tr} follows the $N_{tr} \alpha t^{1/2}$ relation (it will be discussed in the next section). Here, we have to note the similarities between Figures 2 and 4, from which one may suggest that, as the annealing time increases, $\langle a \rangle$ of a photon increases due to void closure between particles in the latex film at the early stage of annealing in which both I_{tr} and N_{tr} start to increase. Later, however, both I_{tr} and N_{tr} saturate by increasing time and $\langle a \rangle$, respectively, by indicating that the void-closure process is completed.

This picture can be visualized by Frenkel's neck formation model[26] which considers the identical contacting spheres under the influence of surface tension. This model assumes that the displaced volume is redistributed uniformly such that the remaining surface keeps their spherical shapes but of larger radii, which offers a larger mean free path, $\langle a \rangle$, of a photon during its journey in the latex film. Figure 6 illustrates Frenkel's picture for the neck-formation process from latex particles. The variation in I_{tr} depends on the mean free path of a photon in the film. At the very early stage of annealing, the photon is refracted or scattered from the particle interfaces, where the mean free path, $\langle a \rangle$, is of the order of the size of the particle or interparticle voids, and after a few steps, it remerges from the front surface of the film [see Fig. 3(a)], which gives rise to high I_{sc} (refs. 14 and 16) and low I_{tr} values. As the viscous flow proceeds, some of the voids disappear and the mean free path becomes of the order of the deformed particle size. Clearly, in this stage, with the same amount of rescattering, a photon can escape from the back surface of the film, and, consequently, I_{tr} increases and I_{sc} decreases.[14,16] Naturally, as $\langle a \rangle$ increases, photons can reach to the back surface easily and $I_{sc}(N_{sc})$ decreases [see Fig. 3(c)].

To support these findings, scanning electron micrographs (SEM) of the latex films before and after annealing at 160 and 180°C for a total of 30 min are presented in Figure 7. In Figure 7(a), one can see individual latex particles in the powder film where many voids can be observed. However, in Figure 7(b,c), SEM images present the void-closure phenomenon due to the annealing of the latex films for 30 min total time at 160 and 180°C, respectively. The films in Figure 7(b,c) present higher I_{tr} intensities than does the film in Figure 7(a), indicating that photons have longer $\langle a \rangle$ values in the former samples, where refraction can occur between deformed particle interfaces.

Void Closure During Film Formation

When the film samples were annealed at 150, 160, 170, 180, 190, and 200°C for 10 min time inter-

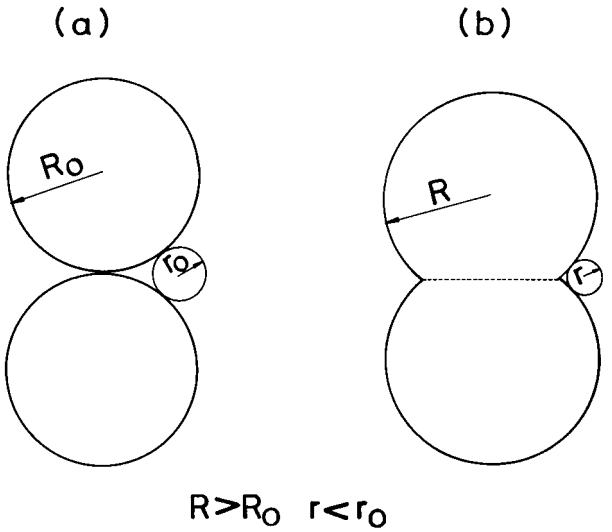

Figure 6 Geometrical illustration of Frenkel's neck growth model between identical particles: (a) before and (b) after neck growth. R_0, R and r_0, r are the particle and void radii before and after neck growth, respectively.

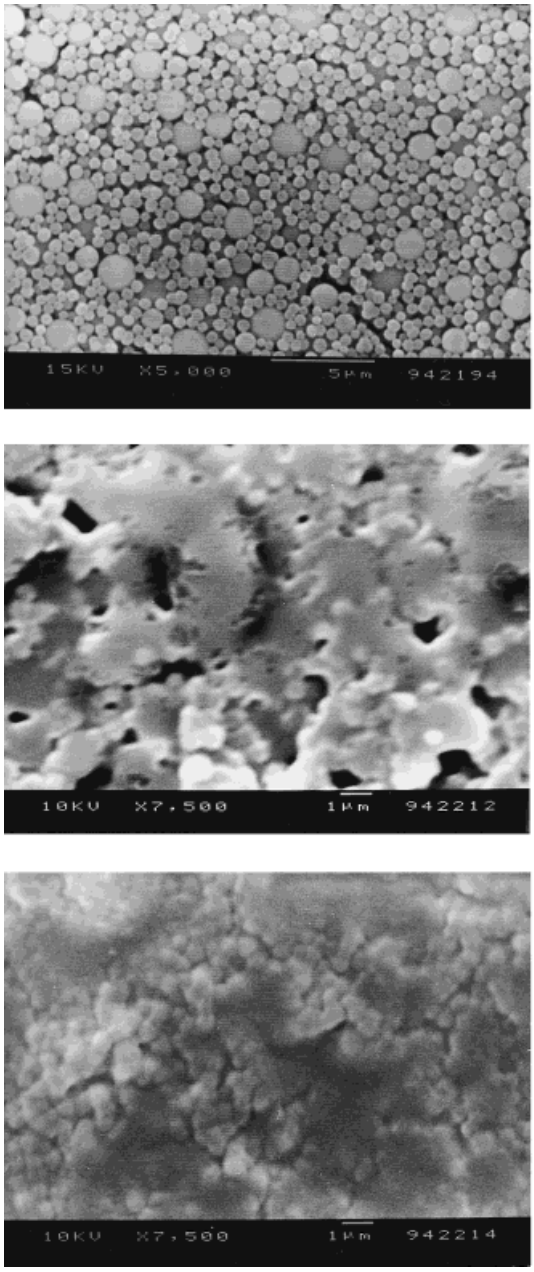

Figure 7 Scanning electron micrographs of latex film samples: (a) before annealing; (b) annealed at 160°C for 3 × 10 min; (c) annealed at 180°C for 3 × 10 min.

vals, a continuous increase in I_{tr} was observed until they were saturated with time, i.e., the clarity of the films approach the asymptotic values. The increase in I_{tr} was explained in the previous sections due to increase in $\langle a \rangle$ of a photon in the latex film because of the disappearance of voids or the void-closure phenomenon.

To quantify the above results, eq. (4) can be used where we assume that the voids are spherical [i.e., $\rho(r)\alpha r^{-3}$]. Then, integration of eq. (4) produces the relation

$$t = \frac{2AC}{\gamma} \exp\left(\frac{B}{T - T_0}\right)\left(\frac{1}{r^2} - \frac{1}{r_0^2}\right) \qquad (5)$$

where C includes the related constant for the relative density, $\rho(r)$.

In the previous section, we stated that as the void radius (r) decreases, the mean free path $\langle a \rangle$ of the photon increases, which then causes an increase in the I_{tr} intensity. Here, an assumption can be made that the I_{tr} intensity is inversely proportional to void radius, r. Then, eq. (5) can be written as

$$t = \frac{2AC}{\gamma} \exp\left(\frac{B}{T - T_0}\right) I_{tr}^2 \qquad (6)$$

where it is naturally considered that the initial radius of the void r_0 is larger than r, which then resulted in the omission of r_0^{-2} compared to r^{-2}. Equation (6) can be solved for I_{tr} to interpret the experimental results as

$$I_{tr} = S(T)t^{1/2} \qquad (7)$$

where

$$S(T) = \left(\frac{\gamma}{2AC}\right)^{1/2} \exp\left(-\frac{B}{2(T - T_0)}\right) \qquad (8)$$

Here, one should notice that our assumption that was made in the previous section where $N_{tr}\alpha t^{1/2}$ was taken is consistent with eq. (7). In Figure 8, I_{tr} values are plotted against $t^{1/2}$ for films annealed at 150, 160, 170, and 180°C. I_{tr} increases linearly for all samples, which indicates that the model chosen for the void-closure mechanism works well for our UVV data. In other words, I_{tr} is linearly dependent on $\langle a \rangle$, which is consistent with our assumption that I_{tr} is inversely proportional to r (i.e., $\langle a \rangle \propto r^1$). The slopes in Figure 8 produce a temperature-dependent parameter $S(T)$ which can also be plotted versus $(T - T_0)^{-1}$ to produce B values according to eq. (8). The logarithmic plot of $S(T)$ versus $(T - T_0)^{-1}$ is shown in Figure 9 which also presents a nice linear relation except for points at 190 and 200 K, indicating that the void-closure model used fits our data quite well. B is found to be 12.8×10^3 K, which is three

times larger than the value obtained for acrylic (4×10^3 K)[27] and 60 times larger than that found for waterborne acrylic lattices.[28] A smaller value for the copolymer of MMA and 2-ethylhexyl acrylate lattices was attributed to the plasticizing effect of water.[17] In our case, no such plasticizing effect is expected, because our PMMA latex has a glass transition of 380 K, which is very high compared to waterborne acrylic lattices ($T_g \approx 280$ K). The value of $B = 12.8 \times 10^3$ K for our system seems to be quite reasonable for our hard latex particles and the measured value of B suggests that heptane has no plasticizing effect on PMMA latex particles. One should have noticed that, while we produce the B value from Figure 9, the points at 190 and 200 K are excluded from the fit. Here, it is believed that at these high temperatures voids in the latex film are immediately filled with the polymeric material at early times of annealing (maybe in 5–10 min), and then equilibration (chain interdiffusion) processes start, i.e., these high-temperature points may correspond to the equilibration regime.

It should also be emphasized that the latex films can at most reach 60% of transparency by annealing at 200°C, which means that these films still contain some structural heterogeneities, i.e., they have not reached their full mechanical strength. From here, the main conclusion can be reached that the time duration and temperature for annealing is quite critical for the formation of strong latex film.

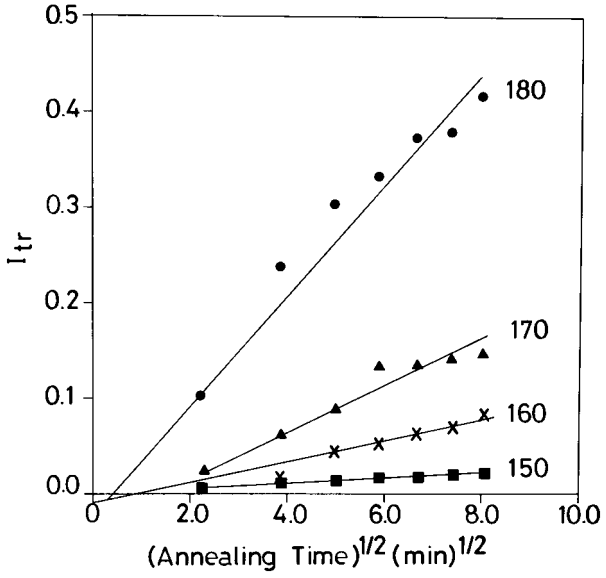

Figure 8 Plot of transmitted photon intensity I_{tr} versus square root of annealing time and fit of data to eq. (7), for various temperatures. Numbers on each curve present the annealing temperatures.

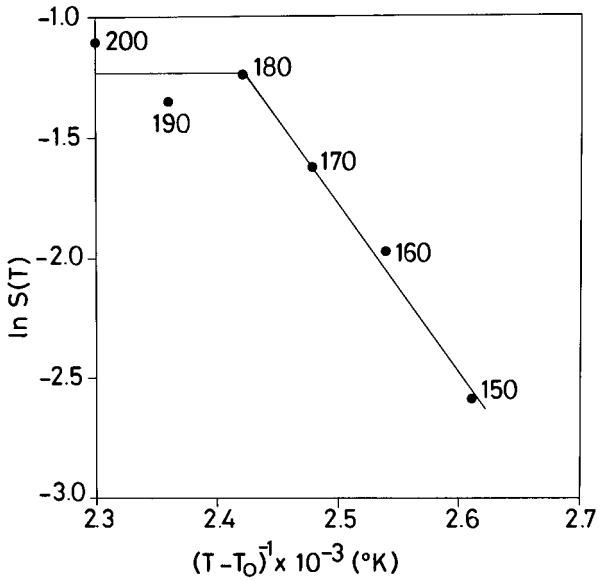

Figure 9 Logarithmic plot of $S(T)$ values versus $(T - T_0)^{-1}$ for the data obtained from Figure 8. The slope of the plot was obtained by fitting the data to eq. (8) which produced B values.

In conclusion, this work has introduced a kinetic model for measuring the viscous flow parameter B for the void-closure process during latex film formation. This model was justified by the Monte Carlo simulations in conjunction with SEM measurements. Further study can be made by increasing the time duration for a given annealing temperature to test the improvement of the transparency of latex films. However, the measured B values would not be affected by the chosen time duration.

We thank Professor M. A. Winnik for supplying us with the latex material and stimulating us with his ideas.

REFERENCES

1. Sperry, P. R.; Snyder, B. S.; O'Dowd, M. L.; Lesko, P. M. Langmuir 1994, 10, 2619.
2. Kausch, H. H.; Tirrell, M. Annu Rev Mater Sci 1989, 19, 341.
3. Mazur, S. in Polymer Powder Technology, Maukis M.; Rosenweig, V., Eds.; Wiley: New York, 1996.
4. Vanderhoff, J. W. Br Polym J 1970, 2, 161.
5. Kanig, G.; Neff, H. Colloid Polym Sci 1975, 256, 1052.
6. Wang, Y.; Kats, A.; Juhue, D.; Winnik, M. A.;

Shivers, R. R.; Dinsdale, C. J. Langmuir 1992, 8, 1435.
7. Roulstone, B. J.; Wilkinson, M. C.; Hearn, J.; Wilson, A. J. Polym Int 1991, 24, 87.
8. Kim, K. D.; Sperling, L. H.; Klein, A. Macromolecules, 1993, 26, 4624.
9. Pekcan, O.; Winnik, M. A.; Croucher, M. D. Macromolecules 1990, 23, 2673.
10. Wang, Y.; Zhao, C. L.; Winnik, M. A. J Chem Phys 1991, 95, 2143.
11. Wang, Y.; Winnik, M. A.; Macromolecules 1993, 26, 3147.
12. Pekcan, O.; Canpolat, M. J Appl Polym Sci 1996, 59, 277.
13. Pekcan, O.; Canpolat, M.; Goçmen, A. Polymer 1993, 34, 3319.
14. Canpolat, M.; Pekcan, O. Polymer 1995, 36, 4433.
15. Pekcan, O. Trends Polym Sci 1994, 2, 236.
16. Canpolat, M.; Pekcan, O. J Polym Sci B Polym Phys 1996, 34, 691.
17. Keddie, J. L.; Meredith, P.; Jones, R. A. L.; Ronald, A. M. Proc ACS 1995.
18. Mackenzie, J. K.; Shuttleworth, R. Proc Phys Soc 1949, 62, 838.
19. Winnik, M. A.; Hua, M. H.; Hongham, B.; Williamson, B.; Croucher, M. D. Macromolecules 1984, 17, 262.
20. Pekcan, O.; Winnik, M. A.; Croucher, M. D. Macromolecules 1994, 17, 262.
21. Pekcan, O.; Winnik, M. A.; Croucher, M. D. Phys Rev Lett 1988, 61, 641.
22. Pekcan, O. Chem Phys Lett 1992, 20, 198.
23. McKenna, G. B. in Comprehensive Polymer Science, Booth C.; Price, C., Ed.; Pergamon Press: Oxford, 1989; Vol. 2.
24. Vogel, H. Z Phys 1925, 22, 645.
25. Fulcher, G. S. J Am Ceram Soc 1925, 8, 339.
26. Frenkel, J. J Phys USSR 1945, 9, 365.
27. Van Krevelen, D. W.; Hoftyser, P. J. Properties of Polymers Their Estimation and Correlation with Chemical Structure; Elsevier: Amsterdam, 1976, p. 343.
28. Keddie, J. L.; Meredith, P.; Jones, R. A. L.; Ronald, A. M. Macromolecules 1995, 28, 2673.